Molecular Neurobiology (2019) 56:7977–7993
https://doi.org/10.1007/s12035-019-1640-0

CNS-Specific Synthesis of Interleukin 23 Induces a Progressive Cerebellar Ataxia and the Accumulation of Both T and B Cells in the Brain: Characterization of a Novel Transgenic Mouse Model

Louisa Nitsch[1] · Julian Zimmermann[1] · Marius Krauthausen[1] · Markus J. Hofer[2] · Raman Saggu[3] · Gabor C. Petzold[1,3] · Michael T. Heneka[1,4] · Daniel R. Getts[5] · Albert Becker[6] · Iain L. Campbell[7] · Marcus Müller[1,7]

Received: 5 March 2019 / Revised: 30 April 2019 / Accepted: 6 May 2019 / Published online: 2 June 2019

Abstract

Interleukin 23 (IL-23) is a key mediator in neuroinflammation in numerous autoimmune diseases including multiple sclerosis (MS). However, the pathophysiology of IL-23 and how it contributes to neuroinflammation is poorly defined. To further clarify the role of IL-23 in CNS inflammation, we generated a transgenic mouse model (GF-IL23) with astrocyte-targeted expression of both IL-23 subunits, IL-23p19, and IL-23p40. These GF-IL23 mice spontaneously develop a progressive ataxic phenotype, which corresponds to cerebellar tissue destruction, and inflammatory infiltrates most prominent in the subarachnoidal and perivascular space. The CNS-cytokine milieu was characterized by numerous inflammatory mediators such as IL-17a and IFNγ. However, the leukocytic infiltrates were surprisingly predominated by B cells. To further examine the impact of the CNS-specific IL-23 synthesis on an additional systemic inflammatory stimulus, we applied the LPS-induced endotoxemia model. Administration of LPS in GF-IL23 mice resulted in early and pronounced microglial activation, enhanced cytokine production and, in sharp contrast to control animals, in the formation of lymphocytic infiltrates. Our model confirms a critical role for IL-23 in the induction of inflammation in the CNS, in particular facilitating the accumulation of lymphocytes in and around the brain. Thereby, CNS-specific synthesis of IL-23 is able to induce a cascade of inflammatory cytokines leading to microglia activation, astrocytosis, and ultimately tissue damage. The presented transgenic model will be a useful tool to further dissect the role of IL-23 in neuroinflammation.

Keywords Autoimmunity · Neuroinflammation · B cells · CNS · IL-23 · LPS

Introduction

Since the initial observation that interleukin 23 (IL-23) rather than the structurally related IL-12 is the critical cytokine contributing to the pathogenesis of autoimmune diseases [1, 2], a plethora of studies have confirmed the findings and characterized the role of IL-23 in a variety of disorders such as inflammatory bowel disease,

Louisa Nitsch and Julian Zimmermann shared authorship

Electronic supplementary material The online version of this article (https://doi.org/10.1007/s12035-019-1640-0) contains supplementary material, which is available to authorized users.

✉ Marcus Müller
marcus_m.mueller@ukb.uni-bonn.de

[1] Department of Neurology, Universitaetsklinikum Bonn, Sigmund-Freud-Str. 25, D-53127 Bonn, Germany

[2] School of Life and Environmental Sciences, Marie Bashir Institute for Infectious Diseases and Biosecurity, Charles Perkins Centre, Bosch Institute, The University of Sydney, Sydney, NSW 2006, Australia

[3] German Center for Neurodegenerative Diseases (DZNE), Sigmund-Freud-Str. 27, D-53127 Bonn, Germany

[4] Clinical Neuroscience Unit, Universitaetsklinikum Bonn, Bonn, Germany

[5] Department of Microbiology-Immunology and Interdepartmental Immunobiology Center, Northwestern University Feinberg School of Medicine, Chicago, IL, USA

[6] Department of Neuropathology, Universitaetsklinikum Bonn, Sigmund-Freud-Str. 25, D-53127 Bonn, Germany

[7] School of Molecular Bioscience, University of Sydney, Sydney, Australia

rheumatoid arthritis, and psoriasis [3–7]. Regarding its role in central nervous system (CNS) diseases, a multitude of studies prove a major role of IL-23 in inflammatory brain disorders such as multiple sclerosis (MS) [8–11]. In mice with deficient expression of the IL-23 receptor (IL-23R) as well as transgenic models with deficient expression of the IL-23 subunits p19 or p40, induction of experimental autoimmune encephalitis (EAE) is not possible, arguing for a key role of this cytokine in autoimmune CNS-inflammation [1, 2]. Furthermore, IL-23-driven IL-17-producing CD4+ T helper 17 (Th17) lymphocytes are capable of transferring EAE in passive transfer studies and accumulate in the CNS during the course of the EAE [12]. Furthermore, levels of IL-23 are increased in serum and cerebrospinal fluid of MS patients [11, 13]. In some MS patients, a single nucleotide polymorphism of the subunit p40 is found, which increases the p40 expression, is important in MS, and associated with younger onset of the disease [8]. Besides CNS-autoimmunity, recent studies propose a role of IL-23 in stroke through its pro-inflammatory function after ischemia [14–18], in the pathogenesis of carotid atherosclerosis [19] and link IL-12/−23 with Alzheimer's disease [20]. Furthermore, host defense mechanisms in infectious diseases of the brain such as West Nile virus appear to be dependent on IL-23 by contributing to homing of leukocytes into infected tissue during West Nile Virus encephalitis [21].

IL-23 belongs to the IL-12 family of cytokines and consists of a unique p19 subunit and a common p40 subunit, shared with IL-12 [22]. The IL-23R is composed of the IL-12Rβ1 component, which binds to the p40 subunit, and the IL-23R unit binding to p19. Stimulation of the receptor leads to phosphorylation of signal transducers and activators of transcription (STAT) 1, 3, 4, and 5 [23]. Antigen-presenting cells like macrophages and dendritic cells produce IL-23 [22, 24]. The cytokine stimulates αβ and γδ T cells and contributes to the differentiation of Th17 lymphocytes, the subtype of T lymphocytes, which are critical for chronic inflammation and autoimmune-mediated diseases such as MS [9]. Th17 cells are detected in MS lesions [10].

Since naive T cells lack the IL-23R, their differentiation into Th17 cells is not completely facilitated by IL-23 stimulation. It is postulated that the early development of Th17 cells is initiated by transforming growth factor β (TGF-β) and IL-6 or IL-21 that stimulate the expression of the IL-23R [25–27]. Th17 cells, mediated by IL-23R signaling, subsequently produce their signature cytokines IL-17A and IL-17F among other cytokines like IL-21, IL-22, tumor necrosis factor α (TNFα), and colony-stimulating factor 2 (GM-CSF). Thereby, in the pathogenesis of autoimmune neuroinflammation, IL-17 and also IL-22 seem to be redundant [28–30]. Mice, deficient for these cytokines, are still susceptible for EAE, although IL-17-deficient mice with a less severe phenotype. In contrast, IL-23-induced GM-CSF has a central and nonredundant function in EAE as GM-CSF-deficient mice are resistant to EAE [31, 32].

Taken together, the impact of IL-23 on neuroinflammatory diseases is without doubt, but the mechanisms how IL-23 is able to modulate these conditions still remains to be further elucidated. To dissect the local role of IL-23 in CNS-inflammation in vivo, we generated a transgenic mouse model with CNS-restricted expression of IL-23 under the transcriptional control of a well-described glial fibrillary acidic protein (GFAP) genomic expression vector [33–36]. We demonstrate that CNS-specific expression of IL-23 leads to a severe brain inflammation with striking perivascular and subarachnoidal accumulation of lymphocytes, including a surprisingly high fraction of B cells. We observed the induction of a cascade of inflammatory cytokines, increased accumulation of leucocytes, and enhanced activation of microglia after systemic administration of LPS.

Materials and Methods

Animals

The generation of transgenic mice with astrocyte-specific expression of particular genes was described in detail previously [33–36]. mRNA was isolated from spleen of mice suffering from EAE at peak clinical disease, and the coding sequence of the p19 and p40 subunit of IL-23 was amplified by qPCR. After amplification, the p19/p40 cDNA fragment was cloned into an expression vector derived from the murine glial fibrillary acidic protein (GFAP) gene and containing a human growth hormone (HGH) polyadenylation signal sequence downstream of the insert [35, 37]. Thereafter, the gene construct was used for microinjection into the germline of (C57Bl/6 x 6C3H/HeN) F1 mice. Genotyping of the transgenic offsprings was performed by PCR of tail DNA. The following primers targeted at the human growth hormone sequence and p19/p40 sequence of the transgenic construct were used: AGGTGCGTTCCTCGTAGAGA (5′) for the p40 subunit of the construct, ACTGAGCCCTTAGT GCCAAC (5′) for the p19 subunit of the construct, and AGGTTGTCTTCCCAACTTGC (3′) for the common HGH sequence of both p40 and p19 constructs. Hemizygote transgenic founder mice were backcrossed to the C57BL/6 genetic background for at least eight generations. All mice were kept under standardized pathogen-free conditions at the animal facility of the University Hospital of Bonn, Germany. Animal experiments were approved by the Animal Care Commission of Nordrhein-Westfalen, Germany.

Clinical Assessment of Mice

Mice were clinically evaluated over at least 24 months. The clinical score for ataxia was assessed according to a previously described score [38, 39]. A cumulative scale of four points was used, giving one point to each of the following symptoms: splayed legs, dragging weight on the trunk rather than on the legs, wobbling, and falling from side to side.

Cytokine and Chemokine mRNA Determination by q-PCR

mRNA was isolated using Trizol reagent (Invitrogen, Darmstadt, Germany). For transcription into cDNA, 1 μg total mRNA was used using SuperScript™ III Reverse Transcriptase (Invitrogen). Real-time quantitative PCR assays were performed using Taqman reagents for the following targets p19, p40 and TNFα, CxCL10, IL1b, CD68 in the LPS-experiments (Applied Biosystems, Darmstadt, Germany). Predesigned PrimePCR 96-well plates (Bio Rad, Munich, Germany) were used to amplify all other targets for transgenic mice $n = 8$ and WT mice $n = 3$. Targets were analyzed in duplicates. Mean mRNA level was normalized to the mRNA level of *GAPDH as the internal control* and expressed in the graphs relative to (untreated) WT controls.

Determination of IL-23 Protein

Level of IL-23 protein was determined by ELISA (R&D Systems, Minneapolis, USA) in supernatant of transgenic and WT brain homogenates ($n = 3$) according to the manufacturer's protocol. A standard curve was generated according to the manufacturer's protocol.

Ultra High-Field MRI

MRI measurements were performed on an 11.7 T horizontal small-bore magnet (Biospec 117/16, Bruker, Germany) using a two-element transmit/receive proton (^{1}H) cryocoil (Bruker Biospin, Germany). Animals were anesthetized by inhalation using isoflurane at 2% for induction on the bench and maintained at 1.0% inside the magnet via tubing within a respiration mask positioned around the animal's snout. Body temperature was maintained at 37 °C via an integrated water heating system and the respiratory rate was maintained at 70–80 cycles per minute. Anatomical images were acquired using a rapid acquisition relaxation enhancement (RARE) T_2-weighted (T_2-w) sequence: echo time (TE) = 0.04 s, repetition time (TR) = 2.5 s, slice thickness 0.5 mm, FOV 1.8 × 1.6 cm and a RARE T_1-weighted (T_1-w) sequence: TE/TR = 0.01 s/1 s, slice thickness 0.5 mm, FOV 1.8 × 1.6 cm.

Routine Histology and Immunohistochemistry

Mice were sacrificed by deep isoflurane anesthesia and transcardially perfused with PBS. Brains were removed, cut along the sagittal midline and, after fixation with PBS-buffered 4% paraformaldehyde, half brains were embedded in paraffin. For cryosections, tissue was embedded in Tissue Tek (Sakura Finetek, Staufen, Germany). Sections (10 μm) were prepared of both paraffin- and cryo-embedded tissue. Paraffin-embedded sections were deparaffinized with xylene, rehydrated in graded ethanol series, and stained with H&E (Sigma-Aldrich, Munich, Germany) and Luxol fast blue for routine histology and analysis of myelination. For immunohistochemistry, slides were incubated over night at 4 °C with the listed primary antibodies (Table 1) after incubation with Proteinase K (ThermoScientific, Waltham, USA; 1:1000) or incubated with biotin-conjugated tomato lectin and washed with PBS. A corresponding biotinylated secondary antibody was used for 45 min (Jackson ImmunoResearch, Newmarket, UK, 1:200) and HRP-coupled streptavidin for another 45 min (Vector Labs, Burlingame, USA; 1:200). For the immunoperoxidase, Nova Red (Vector Labs), as the substrate, was used according to the manufacturer's instruction. Sections were counterstained with hematoxylin (Sigma-Aldrich, Munich, Germany). For Prussian blue staining, slides were deparaffinized and incubated with a 2% potassium ferrocyanide (II) (Sigma-Aldrich, Munich, Germany) and 1% hydrochloric acid solution for 30 min and stained with nuclear fast red (Roth, Karlsruhe, Germany) for 5 min. Frozen sections used for fluorescent immunohistochemistry were incubated with the listed primary antibodies (Table 1) overnight at 4 °C, washed with PBS, and incubated with an A594 or A488 fluorescence-conjugated secondary antibody (Invitrogen, Darmstadt, Germany; 1:400, 45 min). Sections were counterstained with DAPI (Sigma-Aldrich, Munich, Germany). A Nikon eclipse 800 bright-field and fluorescence microscope (Nikon, Düsseldorf, Germany) was used, and bright field and monochrome fluorescent images were captured with a SPOT flex camera and SPOT advanced 4.5 software (Diagnostic instruments, Sterling, USA).

Flow Cytometry

Isolation of microglia and infiltrating leukocytes from the cerebellum was described in detail previously [40]. For removal of intravascular leukocytes, mice were transcardially perfused with 4 °C 1x PBS until the perfusate was clear. The dissected cerebellum was homogenized in Hank's Balanced Salt Solution (HBSS, Gibco, Eggenstein, Germany) using a tissue homogenizer (glass potter, Braun, Melsungen, Germany) before passing

Table 1 Antibodies/lectin used for histology

Antibody/lectin	Specifity	Dilution	
		Paraffin	Cryostat
Polyclonal rabbit anti-Iba1, reactive with human, mouse and rat Iba1 (Wako Chemicals)	Microglia/macrophages		1:500
Monoclonal rat anti- mouse CD68 (Serotec)	Microglia/macrophages		1:250
Polyclonal rabbit anti-laminin, reactive with human and mouse laminin (Sigma-Aldrich)	Basal lamina	1:50	1:50
Biotin-conjugated tomato lectin, *L. esculentum* (Axxora)	Microglia/macrophages, endothelial cells	1:50	
Polyclonal rabbit anti-GFAP (Dako, Hamburg, Germany)	Astrocytes	1:250	
Hamster anti-mouse CD3e (BD Biosciences)	T cells		1:500
Polyclonal rabbit anti-human CD3 (Dako)	T cells	1:200	
Rat anti-mouse CD8a (BD Biosciences)	CD8+ cells		1:200
Rat anti-mouse CD4 (BD Biosciences)	CD4+ cells		1:200
Rat anti-mouse B220 (BD Biosciences)	B cells	1:200	

through a 70-μm cell strainer (BD biosciences, Heidelberg, Germany). After centrifugation, pellets of the homogenates were resuspended in 75% isotonic 4 °C Percoll solution (GE-Healthcare, Uppsala, Sweden) and overlayed with 25% and 0% isotonic Percoll solution. The Percoll density gradient was centrifuged for 25 min, 800 g at 4 °C. Afterwards, microglia, leukocytes, and astrocytes were removed from the 25%/75% Percoll solution interface. After washing with 1x PBS, cells were blocked with CD16/CD32 antibody (Fc block; eBioscience, Frankfurt/Main, Germany) and incubated with fluorochrome-conjugated antibodies (eBioscience; BD Bioscience, Heidelberg, Germany) for detection of CD3e, CD4, CD8a, CD11b, CD45, CD138, NK1.1, Ly6G, and B220. For the intracellular staining, after removal from the Percoll solution interface, the cells were washed and incubated with 50 ng/ml PMA, 1 μmol/ml ionomycin, and brefeldin A 1 μl/1 ml (eBioscience; BD Bioscience, Heidelberg, Germany) for 4 h at 37 °C. After washing with 1x PBS, the cells were blocked with CD16/CD32 antibody (Fc block; eBioscience, Frankfurt/Main, Germany) and incubated with fluorochrome-conjugated antibodies (eBioscience; BD Bioscience, Heidelberg, Germany) for detection of CD4 and CD45. Afterwards, the cells were permeabilized with the fixation/ permeabilization solution kit (eBioscience; BD Bioscience, Heidelberg, Germany) according to the manufacturer's protocol and stained with fluorochrome-conjugated antibodies (eBioscience; BD Bioscience, Heidelberg, Germany) for detection of IL17a and IFNγ. Acquisition was performed with a BD FACSCanto II flow cytometer (BD Biosciences, Heidelberg, Germany). Data were analyzed using the flow cytometry software, FlowJo (TreeStar, San Carlos, CA).

Analysis of Blood Brain Barrier (BBB) Integrity with Evans Blue Dye (EBD)

The integrity of the BBB was described in detail previously [36]. Briefly, 3 h before sacrificing, three transgenic and WT mice were intraperitoneally injected with EBD (2% *w/v* in isotonic NaCl, 4 ml/kg body weight, AppliChem, Darmstadt, Germany). After transcardial perfusion with 4 °C 1x PBS, supplemented with 2 mM EDTA (Sigma-Aldrich, Munich, Germany), forebrain, cerebellum, and liver were washed with double-distilled H2O, weighed, and homogenized in a threefold volume of 50% trichloroacetic acid (w/v, AppliChem, Darmstadt, Germany) solution. After centrifugation, supernatants were diluted with ethanol (1:3), and fluorescence was measured with a microplate fluorescence reader (excitation 620 nm, emission 680 nm) (Tecan infinite 200 M, Crailsheim, Germany). A standard curve was generated based on EBD standards diluted with the same solvent.

Induction of Endotoxemia

Induction of endotoxemia was performed as described previously with modifications [36, 41–43]. In the short-term

LPS-model, 2–3 months old, asymptomatic GF-IL23 transgenic mice and WT littermate controls were intraperitoneally injected with 100 µl saline or 100 µl (300 µg) LPS (*Escherichia coli* 026:B6; Sigma, Munich, Germany) 24 h and 8 h before analysis. For the chronic, long-term model, a double injection of a lower dose LPS (50 µg) on two consecutive days was performed and the mice were analyzed 19 days after LPS-administration. After perfusion with ice-cold PBS, brains were used for routine histology, immunhistochemistry, and qPCR.

Statistical Analysis

qPCR data, ELISA, Evans blue dye extravasation data were calculated by a two-tailed Student's *t* test using GraphPad Prism 5.0 (GraphPad Software, La Jolla, USA) with $p < 0.05$ considered to be significant.

Results

Generation of GF-IL23 Transgenic Mice

To examine the direct impact of IL-23 on neuroinflammation, we generated a mouse model (GF-IL23) with CNS-restricted expression of IL-23 using a well-established transgenic approach with expression of a target cytokine under the transcriptional control of the GFAP promoter [34, 36]. Five founder mice (Table 2), transgenic for both IL-23 subunits p19 and p40, and one mouse with single expression of p19 were detected. Two of the GF-IL23 transgenic founder mice developed an ataxic phenotype, while four of the five founder mice showed cerebellar inflammatory infiltrates (Fig. S1), as described below (Table 2). The "p19-only" founder was clinically asymptomatic and displayed no histological alterations. The founder mouse GF-IL23-20 with a high expression of both p19/p40 mRNA, a clinical and histological phenotype as described below, was backcrossed for at least eight generations to the C57Bl/6 background, and subsequent offsprings were used for further analysis. Expression of the p19 and p40 subunit was confirmed by qPCR in the cerebellum, cerebrum, eye, and to a lower amount in the spinal cord (Fig. 1a). In comparison to IL-23 levels in inflammatory disorders affecting the brain such as systemic LPS-models, cerebellum and cerebrum of the GF-IL23 mice showed an even higher IL-23 production compared to cerebellum and cerebrum of LPS treated WT mice, respectively. The translation of transgenic mRNA into IL-23 protein was detected and confirmed by ELISA from whole brain homogenates (Fig. 1b). Neither the clinical phenotype of GF-IL23 mice nor the histological analysis of organs like the heart, hamstring muscle, lung, kidney, liver, or bowel implicated inflammation or alteration of any other organ beside the CNS documenting the CNS-restricted expression of the transgene (data not shown). Taken together, we generated a transgenic mouse model with astrocyte-targeted expression of IL-23 leading to the production of p19/p40 mRNA and protein in the CNS.

Astrocyte-Specific Expression of IL-23 Induces a Progressive Ataxia

GF-IL23 mice displayed a normal development until the age of 4 months. At the age of 4 months, GF-IL23 mice developed progressive clinical symptoms of cerebellar dysfunction with a gait ataxia and weight loss. The clinical phenotype was monitored by a cumulative scale of four points assessing important features of cerebellar dysfunction. Most of the animals developed severe cerebellar symptoms defined as a score of 2 or above between the age of 9–15 months. After 24 months, more than 95% of the animals were affected showing a moderate to strong cerebellar ataxic phenotype (Fig. 1c). Consistent with the clinical observations, the MRI scans revealed cerebellar tissue impairment as the clinical phenotype had already implied. Respectively, MRI scans showed loss of the physiologic cerebellar structure and T_1-w hypointensities and T_2-w hyperintensities (arrow) in the entire cerebellum (Fig. 1d). In summary, the GF-IL23 model leads to a spontaneous and progressive ataxia and cerebellar destruction.

Table 2 Characterization of GF-IL23 transgenic founder mice

Mouse	Genotype	Transgene expression (p19)	Transgene expression (p40)	Phenotype	Histological features
GF-IL23-13	p19/p40	++	+	–	++
GF-IL23-20	p19/p40	++	++	Ataxia	++
GF-IL23-22	p19/p40	+	+++	Ataxia	+
GF-IL23-43	p19/p40	+	+	–	+
GF-IL23-77	p19/p40	+	++	–	–
GF-p19	p19	+++	–	–	–

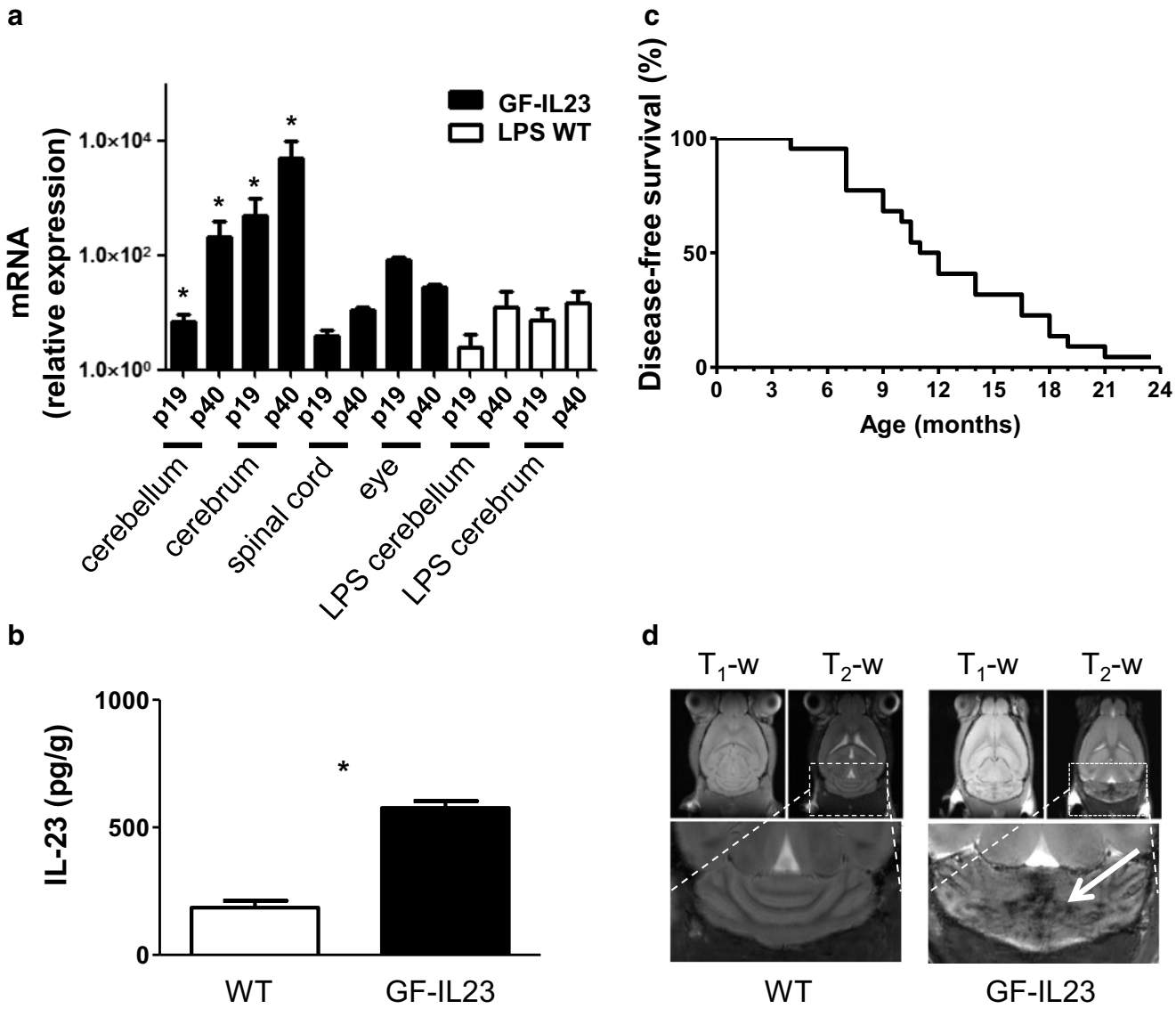

Fig. 1 GF-IL23 mice produce CNS-restricted IL-23 mRNA and protein, thereby presenting an ataxic phenotype and cerebellar lesions in MRI scans. The mRNA level of p19 and p40 of GF-IL23 mice was normalized to GAPDH and expressed relative to WT controls (**a**). Expression of p19 and p40 mRNA in the cerebellum, cerebrum, spinal cord, and eye was increased in GF-IL23 mice ($n = 3$) (**a**). In addition, the mRNA levels of the cerebellum and cerebrum were increased compared to cerebellum and cerebrum of LPS-treated WT animals $*p < 0.05$, respectively (white bars). Besides, the detection of mRNA, the IL-23 protein expression (pg protein/g brain tissue) was confirmed on protein level using an IL-23 specific ELISA assay applied on supernatants of brain homogenates with $*p < 0.05$ (**b**). Kaplan-Meier graph of disease-free survival illustrates the disease onset in GF-IL23 mice ($n = 22$) (**c**). Clinically, GF-IL23 mice showed a progressive ataxia starting at the age of 4 months with peak clinical manifestation after 9–15 months. MRI scans of symptomatic GF-IL23 mice revealed tissue damage of the cerebellum with T_1-w hypointense and T_2-w hyperintense (arrow) lesions in the entire cerebellum (D)

CNS-Restricted Expression of IL-23 Induces Subarachnoidal and Perivascular Infiltrates of Leukocytes and Demyelination in the Cerebellum

Histological analysis of H&E-stained sections from the CNS of symptomatic GF-IL23 mice revealed striking pathological findings in the cerebellar parenchyma and the surrounding subarachnoidal space. In younger transgenic mice with a mild clinical phenotype, few infiltrates were found, surrounding vessels both intraparenchymal and subarachnoidal, but the cerebellar structure was overall maintained (Fig. 2b). In mice with advanced ataxia (Fig. 2c and higher magnification Fig. 2d–f), the infiltrates increased in size and particular in number. Lymphocytes accumulated not only in the perivascular space but also infiltrated the parenchyma. In areas with a high amount of infiltrates, structural tissue damage and

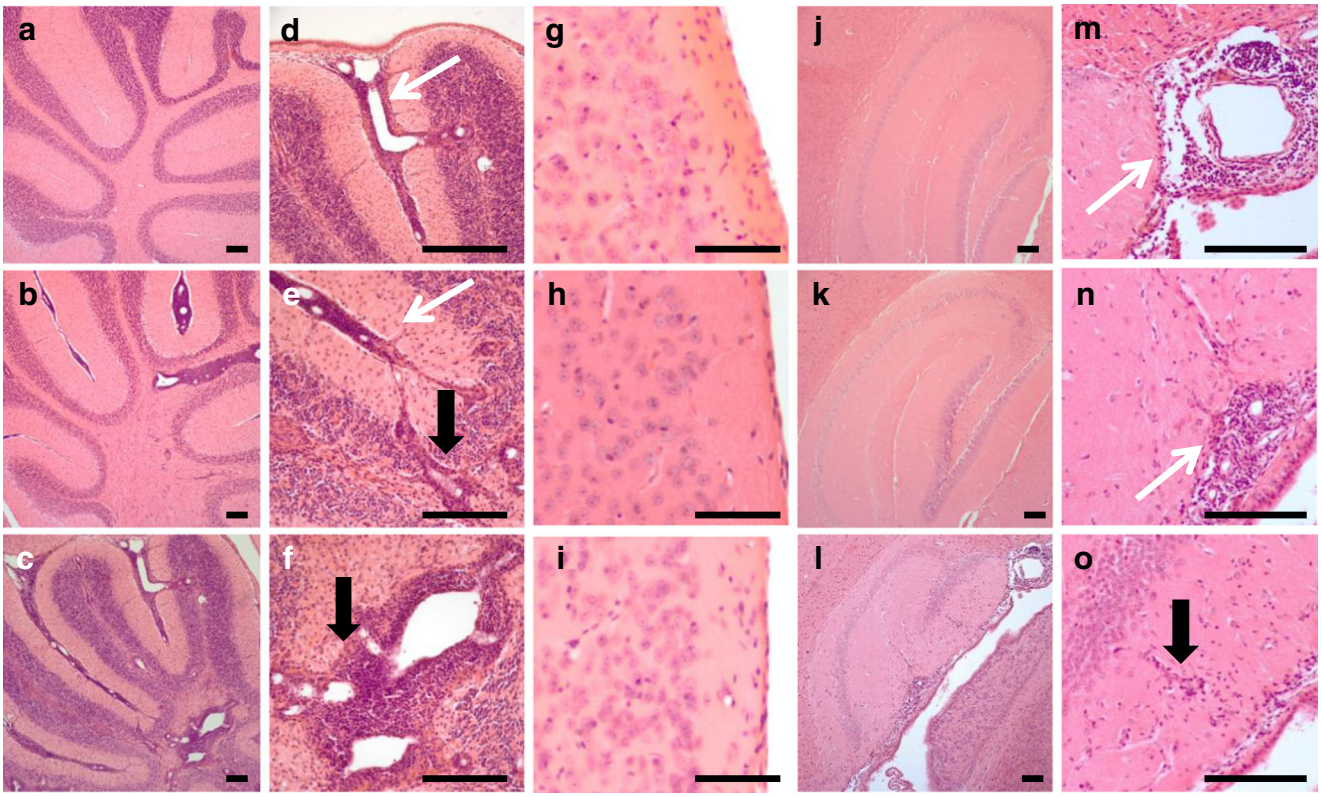

Fig. 2 CNS-specific expression of IL-23 leads to cerebellar infiltrates with perivascular and subarachnoidal accumulation of lymphocytes H&E-staining of cerebellum (**a**–**c**), cerebrum (**g**–**i**), and hippocampus (**j**–**l**) of WT (**a**, **g**, **j**), GF-IL23 mice with few cerebellar infiltrates at early stage disease (**b**, **h**, **k**), and GF-IL23 with highly infiltrated cerebellum at later stage (**c**, **i**, **l**). The cerebellum revealed subarachnoidal and perivascular infiltrates in GF-IL23 mice in comparison to WT mice. Routine histology of the hippocampus detected little intraparenchymal infiltrates and few subarachnoidal infiltrates near the hippocampus of later stage GF-IL23 mice, whereas no infiltration was seen in the hippocampus of WT and early stage transgenic mice. In the cerebrum, no major infiltration or alteration in WT, early stage, and late stage GF-IL23 mice was visible. **d**–**f** Higher magnification of **c**. **m**–**o**. Higher magnification of **l**. White arrows point at subarachnoidal infiltrates, black arrows at perivascular infiltrates. Data are representative for at least $n = 15$ GF-IL23 mice and WT mice. Scale bar 100 μm (**a**, **b**, **c**, **d**, **e**, **f**, **j**, **k**, l, **m**, **n**, **o**) or bar 50 μm (**g**, **h**, **i**)

demyelination could be detected. GF-IL23 mice displayed no major alteration of the cerebral cortex (Fig. 2h, i). Nevertheless, the subarachnoidal space and the parenchyma near the hippocampus in advanced stage mice was slightly infiltrated (Fig. 2l, higher magnification Fig. 2m–o). No infiltrates were detected in WT control littermates (Fig. 2a–j). Whereas in moderate infiltrated tissue of early stage mice, no major demyelination is apparent (Fig. 3b, higher magnification Fig. 3e); in GF-IL23 mice with late stage, long-standing cerebellar symptoms, LFB staining revealed demyelination (Fig. 3c, f), not only restricted to the area of perivascular infiltrated tissue, but nearly in the entire cerebellum. Taken together, CNS-restricted expression of IL-23 led to diffuse demyelination and subarachnoidal and intraparenchymal infiltration of the cerebellum. Thereby, leukocytes mainly accumulate in perivascular infiltrates, but at later stage also more diffusely independent from vascular structures. The findings of mainly cerebellar lesions were congruent with the clinical observation and MRI data described in Fig. 1.

Astrocytosis and Microglial Activation in GF-IL23 Mice

In areas of inflammatory infiltrates, GFAP staining detected astrocytes with a prominent cell body and hypertrophic processes in GF-IL23 mice (Fig. 3h, i). Microglial morphology and activation were further analyzed by lectin histochemistry. Whereas the cerebellum of GF-IL23 mice displayed activated microglia with hypertrophic cell bodies much enhanced at late stage (3 l), microglia of WT mice were typically resting and ramified (Fig. 3j). Thus, the CNS restricted expression of IL-23 led to astrocytosis and microglia activation.

The Accumulation of Lymphocytes Includes a High Proportion of B Cells

Immunhistochemistry against CD3, CD4, CD8, and B220 was used to discriminate between T cell subsets and B cells. The infiltrates comprised of a high proportion of B cells both in highly infiltrated tissue (Fig. 4a) and in smaller infiltrates

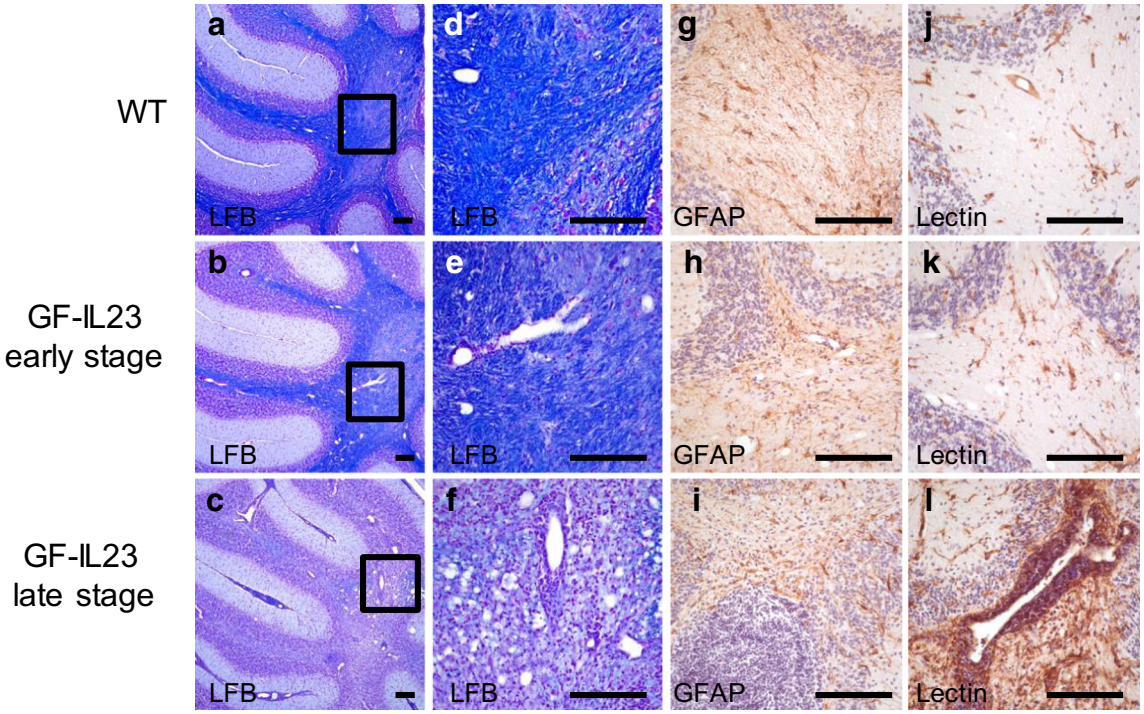

Fig. 3 Astrocyte specific expression of IL-23 leads to demyelination and activation of microglia and astrocytes (**a**–**f**) LFB staining showed demyelination in the cerebellum of GF-IL23 mice in early stage (**b**, **e**) and especially in highly infiltrated cerebellum of GF-IL23 mice (**c**, **f**) compared to WT (**a**, **d**). Anti- GFAP staining (**g**, **h**, **i**) and tomato-lectin- staining (**j**, **k**, **l**) exhibited activation of astrocytes and microglia increasing with the amount of infiltration (WT **g**, **j**; GF-IL23 mice early stage **h**, **k**; late stage **i**, **l**). Representative data of at least $n = 6$ mice for each genotype. Scale bar 100 μm

(Fig. 4b) at early stage disease, whereas the proportion of CD3+ T cells appeared much smaller and not entirely restricted to the perivascular infiltrates. CD3+ T cells showed a more diffuse distribution leaving the perivascular structures and infiltrating the parenchyma (Fig. 4c, d). Fluorescence immunohistochemistry with double staining of B and T cells indicated that some infiltrates had a diffuse distribution of B and T cells (Fig. 4e), while others had a more restricted B and T cells

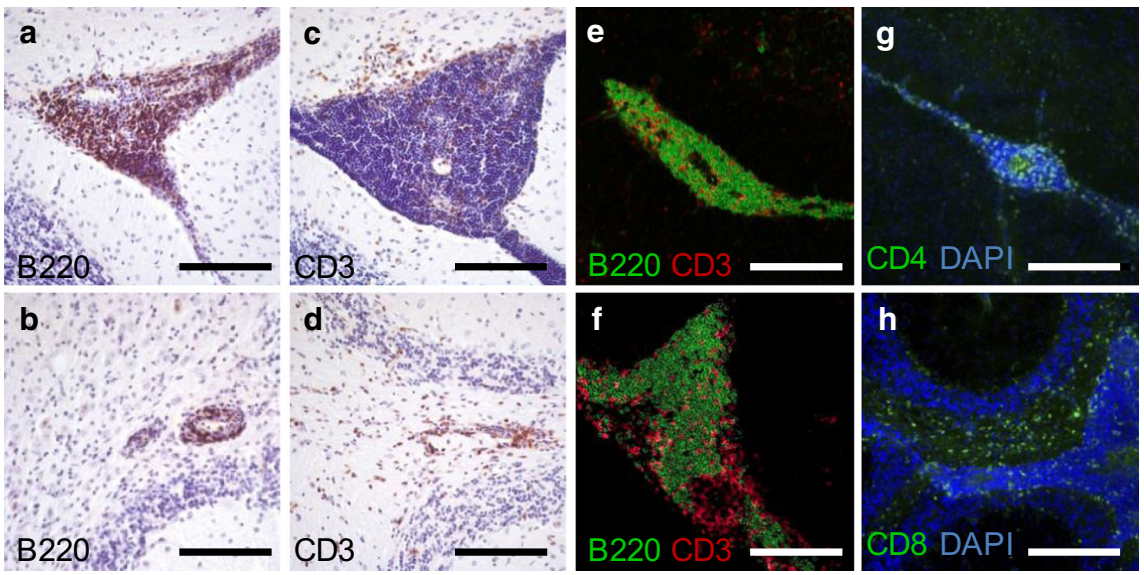

Fig. 4 IL-23 leads to accumulation of B and T cells. Immunohistochemistry revealed accumulation of B220+ cells (**a**, **b**) and CD3+ cells (**c**, **d**) in GF-IL23 mice in highly infiltrated tissue (**a**, **c**) as well as in milder infiltrated cerebellum (**b**, **d**). Immunohistochemistry of frozen sections of GF-IL23 mice for B220, CD3 (**e**, **f**), CD4 (**g**), CD8 (**h**) revealed the distribution of B and T cells among the infiltrates. Data are representative for at least $n = 6$ GF-IL23 mice and WT mice. Scale bar 100 μm

area (Fig. 4f). Among the T cells, CD4+ cells follow the vascular structures (Fig. 4g), whereas CD8+ cells diffusely infiltrated the surrounding tissue (Fig. 4h).

Perivascular Accumulation of Hemosiderophages and Cerebellar Disruption of the Blood Brain Barrier

The histological evaluation of brain tissue and the subarachnoidal space from GF-IL23 mice infrequently revealed erythrocytes in close proximity of vessels. In addition, we constantly detected pigmented cells in proximity to small vessels and infiltrates which resembled the histological features of hemosiderophages. Prussian blue staining confirmed these findings with hemosiderin-loaded cells, which were predominant in vascular walls next to the infiltrates. The amount of detected hemosiderophages correlated with the age and amount of tissue destruction (Fig. 5a–d). To evaluate the impact of IL-23 on the integrity of the blood brain barrier (BBB), we systemically applied Evans Blue dye. Whereas in the cerebrum of WT and transgenic mice no significant extravasation of the dye was seen, the cerebellum of transgenic mice revealed up to fivefold increased measurements of the dye in the homogenates compared to WT cerebellum indicating a disruption of the BBB in the transgenic cerebellum. Liver tissue served in this experiment as a positive control with physiological extravasation of the dye (Fig. 5e). In conclusion, the transgenic model induced microbleedings in the cerebellum and disruption of the blood brain barrier.

Phenotypic Characterization of Cerebral Leukocytes in GF-IL23 Mice by Flow Cytometry

To further examine the cellular composition of the detected inflammatory infiltrates, flow cytometric analysis was performed. FACS data confirmed the infiltrates in the brains of the transgenic mice mainly consisted of lymphocytes with a high percentage of B cells beside CD3+ cells (Fig. 6a). Among the CD3+ cells, both CD4+ and CD8+ cells were found in an equal distribution (Fig. 6b), whereas natural killer cells, dendritic cells, and granulocytes with about 2–3% of all CD45+ cells were only mildly increased (Table 3). The amount of γδ-T cells was not significantly elevated. In addition, GF-IL23 mice showed an increase in $CD11b^{high}$/ $CD45^{high}$ surface expression compared to WT controls indicating activated microglia and/ or infiltrating macrophages in the cerebellum (Fig. 6c). For Th1 and Th17 T cell differentiation, we analyzed the intracellular IFNγ and IL17a production in CD4+ cells. Despite the presence of IL-23, we found that most CD4+ cells were IFNγ positive, and only few were positive for IL-17a arguing for a dominant Th1 response (Fig. 6d). In addition a small proportion of CD4+ cells expressed both IL17a and IFNγ. Among the B cells, few plasmablasts ($B220^{high}CD138^{+}$) and plasmacells ($B220^{low}CD138^{+}$) were detected in the cerebellum (Fig. 6e). Furthermore, we found follicular ($CD21^{int}CD23^{high}$) and marginal zone ($CD21^{high}CD23^{low}$) B cells in the

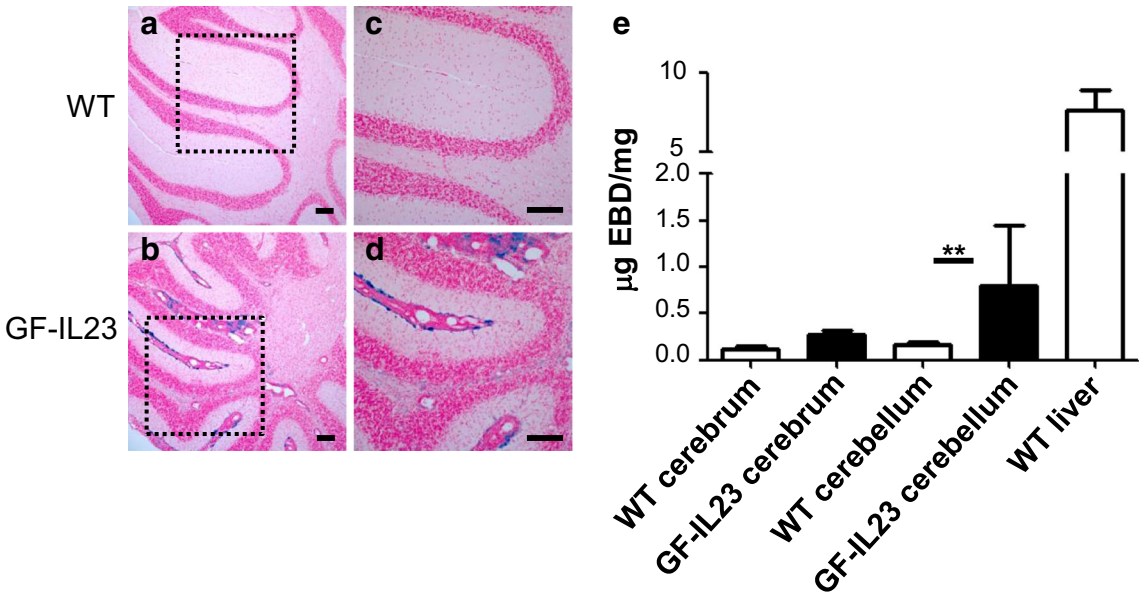

Fig. 5 GF-IL23 mice show perivascular accumulation of hemosiderophages and slight disruption of the blood brain barrier. Cerebellum WT, 20 months of age (**a**, **c**) and GF-IL23, 20 months was compared (**b**, **d**). Prussian blue staining of paraffin-embedded sections detected hemosiderin-loaded cells around the vessels of GF-IL23. For examination of the integrity of the blood brain barrier, Evans blue dye extravasation into cerebrum and cerebellum was analyzed for $n = 3$ WT an $n = 3$ transgenic mice (**e**). Liver tissue served as a positive control. Data revealed extravasation of Evans blue dye into cerebellum of GF-IL23 mice whereas no extravasation in the cerebrum was observed (**$p < 0.005$). Scale bar 100 µm

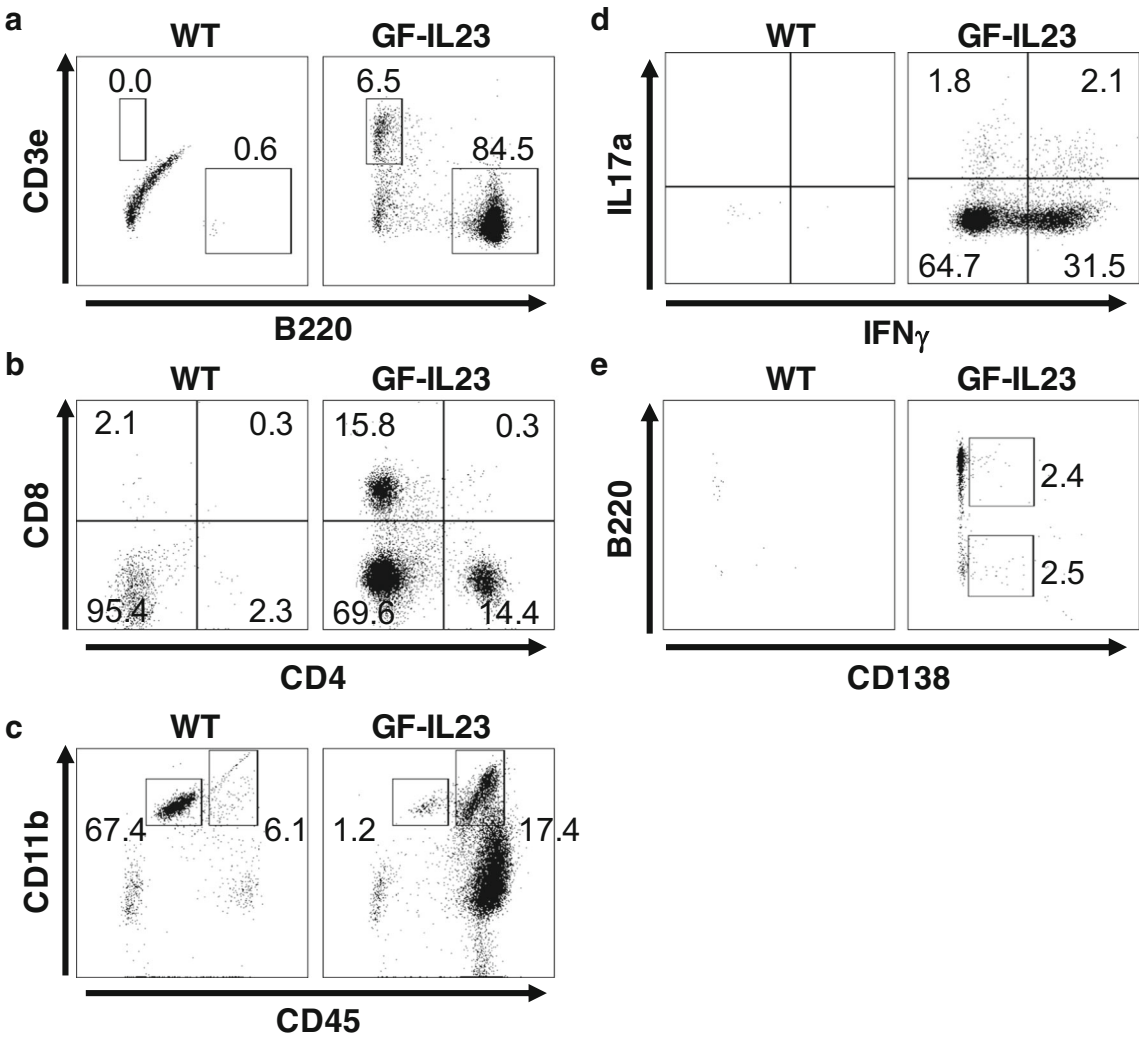

Fig. 6 GF-IL23 mice show infiltration of B cells, T cells, and activated microglia/macrophages. Representative flow cytometry profiles of the cerebellum of GF-IL23 and WT mice. Single cell suspensions from the cerebellum of WT and GF-IL23 mice were stained against B220, CD3, CD4, CD8, CD11b, CD45, IL17a, IFNγ. **a**, **b** Astrocyte-specific expression of IL-23 among leukocyte CD45+ gated cells led to an increased population of B cells, $CD3^+$, $CD4^+$, $CD8^+$ cells, and (**c**) induced a population of $CD45^{high}/CD11b^{high}$-activated microglia/macrophages in the GF-IL23 mice. In the cerebellum of GF-IL23 mice few Th17 cells, but also a strong accumulation of Th1 cells (**d**) was found in CD4+ gated cells. Plasmablasts and plasmacells were detected in the cerebellum of transgenic mice (**e**) in CD19+ gated cells. Data are representative for at least $n = 6$ for each genotype

cerebellum. We did not find a relevant B1 B cell population ($B220^{int}CD5^{int}$) (Fig. S2). In addition, the B cells were slightly activated regarding CD19 expression and slight upregulation of CD80 and CD86 expression (compared to spleen) (Fig. S2). Concerning the expression of IgD and IgM on CD19+ cells, we found early (IgM + IgD-), mid (IgM + IgD+), and late (IgM-IgD+)-activated B cells. Compared to the spleen, we found a significant decrease of IgM + IgD+ B cells, while the proportion of mature IgM-IgD- B cells was increased, maybe containing class switched cells. In summary, the flow cytometry data confirmed and further specified the histological finding of cerebellar leukocyte accumulation with high proportions of T and in particular B cells in GF-IL23 transgenic mice. We predominantly found Th1 as well as a smaller proportion of Th17 cells and IL17a/IFNγ double expressing cells. Data of B cell differentiation revealed few plasmablasts and plasmacells in the cerebellum of GF-IL23+ mice.

Cerebral IL-23 Expression Induces a Cascade of Proinflammatory Cytokines

We next examined the impact of astrocytic IL-23 synthesis on the local inflammatory milieu by qPCR. We found a striking mRNA-upregulation of all examined cyto- and chemokines arguing for the induction of a proinflammatory cytokine cascade. The results are summarized in Fig. 7. Data indicated a proinflammatory milieu with 10- to 1000-fold upregulation compared to wild type controls of classical proinflammatory cytokines like

Table 3 FACS quantification of infiltrating leukocytes in GF-IL23 mice and controls relative to all CD45 positive cells. Indicated are mean values (% of CD45+ cells) and standard deviation with *p< 0.05

	γδ TCR (γδTCR$^+$/ CD45$^+$)	NK cells (NK1.1$^+$/ CD45$^+$)	Dendritic cells (CD11c$^+$/ CD45$^+$)	Granulocytes (Ly6G$^+$/ CD45$^+$)
GF-IL23	0.6%	2.0%*	2.5%*	2.7%*
	−/+ 0.5	*−/+ 0.6*	*−/+ 0.7*	*−/+ 1.8*
WT	0.3%	0.9%	1.1%	0.5%
	−/+ 0.2	*−/+ 0.9*	*−/+0.7*	*−/+ 0.3*

TNFα, IL12, IL1α, IL1β, IL6, as well as Lipocalin 2. The Th1 cytokines IFNγ, IL2, and the Th17 cytokine IL17 were raised as well as the inducible chemokines CCL19, CXCL13, and the CXCR3 ligands CXCL9, CXCL10 were (Fig. 7a). Regarding the cytokine receptors, CXCR3 and CCR7 were prominently elevated (Fig. 7b). In addition, qRT PCR data displayed high expression of the cell surface molecules CD4, CD8, and CD19 and the cell marker/activation markers CD11b/CD68 (Fig. 7c). There was likewise a pronounced induction of several lymphocyte activation markers such as CD80, CD86, CD68, and MHCII (Fig. 7c). To conclude, the mRNA findings corroborated the histological findings and the FACS data and implicate a striking impact of IL-23 towards a highly proinflammatoy cytokine milieu in the cerebellum.

Enhanced Microglia Activation After LPS-Induced Systemic Endotoxemia

After characterizing the spontaneous inflammatory effect of IL-23 in GF-IL23 mice, we questioned if IL-23 would enhance the local immune response in the CNS after a systemic proinflammatory stimulus. To address this question, we applied the LPS-induced endotoxemia model, which provokes a considerably enhanced inflammatory reaction of the brain [36, 41]. For these experiments, 2–3 months old, asymptomatic GF-IL23 mice were analyzed. At this age, GF-IL23 transgenic mice did not show any morphological abnormalities, in particular, no inflammation. First, we analyzed the effect in a short-term LPS-model. The cerebellum was analyzed 24 h after dual administration of LPS. In the routine histology, GF-IL23 mice showed minor perivascular infiltrates after LPS-injection compared to WT and transgenic sham controls which did not show any perivascular infiltrates (Fig. 8a–d). Histology staining for tomato lectin of LPS-treated GF-IL23 mice revealed a pronounced microglial activation when compared to WT and GF-IL23 sham controls (Fig. 8e–h). This finding was corroborated by a significantly enhanced mRNA expression of the microglial activation marker CD68 in the cerebellum of GF-IL23 mice, whereas other relevant cytokines like TNFα, IL1b, and CXCL10 were not increased in the short-term LPS-model (Fig. 8i). To examine the long-term impact of LPS-induced neuroinflammation in GF-IL23

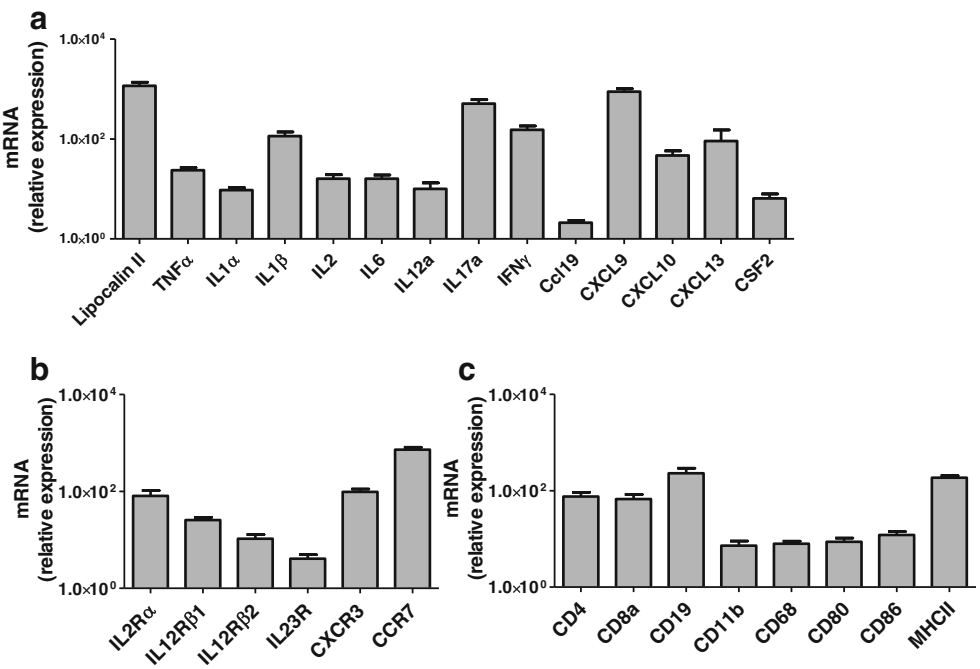

Fig. 7 Cerebral IL-23 expression leads to induction of proinflammatory and activation marker. The mRNA level of certain proinflammatory and activation marker of GF-IL23 ($n = 7$) was normalized to GAPDH and expressed relative to WT controls ($n = 3$). qPCR data revealed induction of several cell markers, as well as proinflammatory and activation markers in the cerebellum of GF-IL23 compared to WT mice (**a**–**c**)

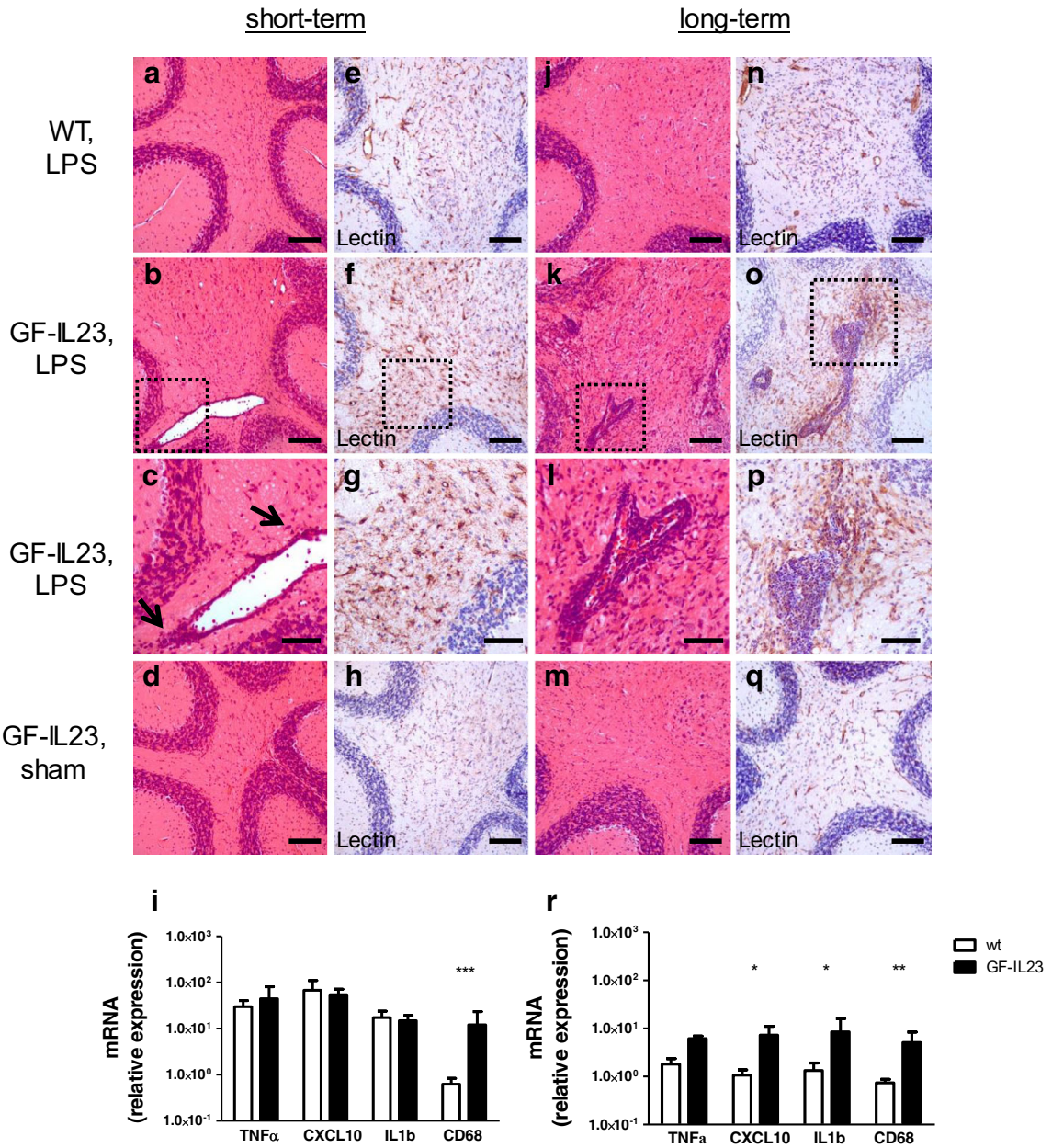

Fig. 8 IL-23 augments microglial activation and increases expression of proinflammatory cytokines after systemic LPS-induced endotoxemia. Routine histological staining (H&E) showed infiltrates in the GF-IL23 short-term LPS mice (**b** higher magnification, **c** arrow pointing to the infiltrates) and to a higher amount in the chronic GF-IL23 LPS-model (**k**, higher magnification, **l**) compared to WT LPS-treated (**a**, **j**) and GF-IL23 sham-treated mice (**d**, **m**). Tomato-lectin-staining in the cerebellum revealed activated microglia with rounded cell bodies and microglial clustering in the short-term (**f**, higher magnification **g**) and pronounced in the long-term LPS-experiment (**o**, higher magnification **p**) in GF-IL23 LPS mice compared to WT LPS-treated (**e**, **n**) and GF-IL23 sham-treated mice (**h**, **q**). qPCR data, expressed relative to WT controls, exhibited enhanced expression of certain cytokines, and activation markers like CXCL10, IL1b, CD68 in the long-term LPS-treatment in GF-IL23 mice (**r**), whereas except for CD68, no difference between GF-IL23 and WT mice was observed in the short-term experiment (**i**). Data are representative for $n = 3$ WT/GF-IL23 mice with $*p < 0.05$, $**p < 0.005$ $***p < 0.0005$. Scale bar 100 μm (**a**, **b**, **d**, **e**, **f**, **h**, **j**, **k**, **m**, **n**, **o**, **q**) or 50 μm (**c**, **g**, **l**, **p**)

mice, we analyzed a cohort 19 days after LPS-injections (Fig. 8j–r). We found a striking increase of the amount of lymphocyte infiltrates in the cerebellum of transgenic mice after LPS-injection (Fig. 8k, l) compared with age-matched sham-treated GF-IL23 (Fig. 8 m) and WT LPS-controls (Fig. 8j). Consistent with these findings, the microglial activation was even more prominent in the LPS-treated GF-IL23 mice (Fig. 8n–q). Data of qPCR in the chronic LPS-stimulation model showed a significant induction of several proinflammatory cytokines and activation markers such as CXCL10, IL1b, and CD68 in the CNS of GF-IL23 mice (Fig. 8r). In summary, the data from the LPS-experiments demonstrate an augmented immune

response with increased immune infiltration, activation of microglia, and cytokine expression after a systemic LPS-stimulus in GF-IL23 mice.

Discussion

Recent data demonstrate a critical role and local upregulation of IL-23 in autoimmune CNS inflammation [8, 9, 11]. Still, the detailed function of IL-23 during the disease course has not been characterized yet. To further elucidate the role of IL-23 in neuroinflammation, we generated a transgenic model with astrocyte-restricted expression of IL-23. We used a well-established GFAP-targeted expression system [36, 37] and were able to create founder animals with cerebral production of both p19 and p40 mRNA and a prominent CNS-restricted IL-23 protein synthesis.

The established transgenic GF-IL23 mouse model developed a neurological phenotype with a progressive cerebellar dysfunction. The symptoms resembled the phenotype observed in another transgenic mouse model with a CNS-expression of the prototypical Th1 cytokine IL-12 (GF-IL12 mice) [35]. The MRI data and the histological analysis of the GF-IL23 model confirmed cerebellar tissue damage with accumulation of inflammatory infiltrates. Over time, these infiltrates increased in size and number and were accompanied by a glial activation, tissue destruction, and demyelination. When characterizing the cellular composition of the infiltrates, we detected a surprisingly high proportion of B cells in both parenchymal and subarachnoidal infiltrates. This is in contrast to most other mouse models of autoimmune inflammation of the CNS including GF-IL12 mice. IL-12 expression in GF-IL12 mice induces a vast accumulation of T cells and NK cells but not B cells. In addition, GF-IL12 mice but not GF-23 mice develop severe cerebellar calcification further underlining the histopathological differences between IL-12 and IL-23-driven neuroinflammation [35].

The finding of a prominent B cell accumulation points towards an unexpected role of IL-23 in attracting or accumulating B cells into the subarachnoidal space and into the CNS parenchyma. The accumulation of B cells is a well-described pathological feature of MS and a central role of B cells in the pathogenesis of MS and was further substantiated by the positive effect of B cell depleting therapies on the disease course [44–46]. B cells can modulate CNS inflammation by different mechanisms like antibody production, interaction, and costimulation of T cells, which can also be seen in animal models of neuroinflammatory diseases. An EAE model with expression of a T cell receptor specific for the MOG peptide 92–106 in the context of MHC class II leads to spontaneous development of relapsing remitting EAE [47]. These mice are transgenic for the TCR without transgenic MOG specific B cells, though during the disease, expanded autoreactive B cells produce pathogenic antibodies against MOG epitopes, which enhance the demyelinating EAE episodes. Therefore, autoreactive T cells seem to interact with endogenous B cells and lead to expansion of MOG-specific B cells. The site of interaction and the mechanisms are not defined yet. It may occur in the CNS, where infiltrated T cells create an immune milieu, leading to infiltration and activation of naive B cells. Alternatively, activation and expansion of B cells may take place in the periphery, in lymphoid organs like cervical lymph nodes, and spleen, and infiltration of B cells into the CNS takes place afterwards [47]. B cells have essential functions as antibody-producing cells and antigen-presenting cells, can load antigen fragments on to MHC class II molecules, and upregulate costimulatory molecules leading to T cell activation [48–50]. Taken together, B cell functions in autoimmune inflammation of the CNS are very relevant but complex and not well defined yet. The B cell response observed in our GF-IL23 model might resemble some B cell-mediated aspects of neuroinflammation and could therefore be a valuable tool to study these disease aspects, in particular the interaction of B and T cells during CNS inflammation.

We characterized the amount of B cells, the immune infiltrates, and tissue damage at different ages of GF-IL23 mice and could observe that the accumulation of lymphocytes precedes the tissue damage. This is in contrast to the IL-12 expressing GF-IL12 mice, where immune infiltration of mainly CD4+, CD8+ T cells, and NK cells into the CNS is always accompanied by tissue damage.

Striking differences between GF-IL12 and GF-IL23 mice were also revealed by determining the local cytokine milieu as determined by qPCR. Whereas IL-12 induces a strong Th1-polarized cytokine response with very high levels of IFNγ [35], the cytokine pattern detected in GF-IL23 mice was much broader. Both IFNγ and IL17a were highly expressed and likely mediated the observed tissue damage together with pro-inflammatory cytokines like TNFα and IL1. In addition, we noted a high expression of IL-6 in GF-IL23 mice, which may further contribute to the differentiation of Th17 cells. Concerning the induction of chemokines in GF-IL23 mice, the detection of increased levels of CXCL13-RNA is of particular interest. CXCL13 is intimately involved in B cell trafficking [51] and could be a key cytokine in promoting the observed B cell accumulation in the brains of GF-IL23 mice. Overexpression of CXCL13 in peripheral tissue leads to B cell aggregate formation [52]. In addition, a recent study provided evidence that CXCL13 is specifically involved in the CNS accumulation of differentiated B cells [53]. Furthermore, IL-23 induces multiple cellular activation markers like CD68 and the B cell co-stimulatory markers CD40, CD80, and CD86 further corroborating the finding of a highly proinflammatory milieu with infiltration of immune cells into the CNS.

Immune cells and their state of activation were further examined by flow cytometry. The FACS data confirmed the infiltration of CD4+, CD8+, and B cells, and the increase of a $CD11b^{high}CD45^{high}$-activated microglia/macrophage population. Interestingly, among the B cells, we found follicular and marginal zone B cells and few differentiated, CD138+ plasmablasts and plasmacells reflecting antibody producing cells. In addition, the B cells seem to be activated. Though, only few studies describe the interaction of the IL-23/Th17 axis with B cells. Th17 cells are able to induce a proliferative B cell response and antibody production and contribute to the germinal center formation [54]. IL-23-activated Th17 cells modulate normal plasma cell functions and are critical in enhancing the inflammatory activity of newly generated autoantibodies [55]. Beside T cells, a small proportion of B cells and plasma cells express IL-23R as well, thereby directly respond to IL-23 [56, 57].

As IL-23 is well described as a key cytokine in polarizing T cells towards a Th17 phenotype, we further characterized CD4+ cells by their expression of IFNγ as a marker for a Th1 phenotype and IL17a as a marker for a Th17 phenotype. Unexpectedly, we found a large number of IFNγ+ CD4+ cells as well as some IL17a + CD4+ cells and even IL17a + IFNγ+ polyfunctional T cells. The IFNγ+ single expressing CD4+ cell population could be due to the elevated IL-12 level in the cerebellum leading to Th1 cell accumulation. But these findings could also suggest that the local expression of IL-23 by astrocytes is able to either activate T cells towards a Th1 and Th17 phenotype or at least to attract both, activated Th1 and Th17 cells, into the CNS. But the strong IFNγ+ single expressing CD4+ cell population in our model could also be due to the plasticity of the Th17 cells and imply Th1-like cells, meaning ex-Th17 cells. These T cell subsets were described in the context of EAE and murine colitis models [58–60]. Thereby, IL-23 signaling is critical for the terminal differentiation of these cell populations [59, 61]. The presence of IL17a + IFNγ+ double expressing T cells could also be explained by this plasticity of the Th17 cells expressing both cytokines while converting from a Th17 to a Th1 phenotype. IL-23 can promote this conversion by the induction of T-bet in Th17 cells [57]. In several studies, these IL17a + IFNγ+ polyfunctional T cells have been described in EAE models [59, 61, 62].

Furthermore, the histological analysis of the GF-IL23 mice revealed increased iron deposition in the cerebellum. Hemosiderophages, located nearby vessels and in vascular walls in close proximity to the infiltrates, point towards microhaemorrhages and suggest an additional vascular pathology. Interestingly, GF-IL17 mice show a vascular phenotype with capillary rarefaction too, and our phenotype may be linked to the increased IL-17a levels in the CNS of the GF-IL23 [36]. In addition, the GF-IL23 mice displayed a disruption of the blood brain barrier, which is likely the consequence of the severe inflammatory response and not necessary directly mediated by GF-IL23. GF-IL17 mice do not display such a severe inflammatory response and keep an intact blood brain barrier [36].

To examine the impact of IL-23 on the local inflammatory milieu after a systemic immune stimulus in GF-IL23 mice, we applied a systemic acute and a chronic LPS-challenge, often used as an endotoxemia model, in our GF-IL23 model. The acute LPS-stimulus led to a pronounced microglial activation as revealed by lectin histochemistry. Glial activation after acute LPS-endotoxemia in wild type mice is well described [63], but was strikingly enhanced in GF-IL23 mice. These young GF-IL23 mice did not feature lymphocyte infiltrates before the application of LPS; therefore, the observed glial activation is likely mediated by the local inflammatory milieu induced by the transgenic IL-23 and not indirectly by infiltrating lymphocytes. Microglia activation in response to IL-23 was described before [64]. Furthermore, Sonobe and colleagues found IL-23R expression in activated microglia in vitro [65], which should enable these cells to even directly interact with IL-23. We have not analyzed yet, if microglia in the GF-IL23 model actually expresses the IL-23R. Future studies will include analysis of microglia IL-23R expression in the GF-IL23 model. In addition, we cannot ensure that the findings in the lectin histochemistry are actually activated microglia, and we cannot exclude that the findings are related to recruited macrophages in the cerebellum of GF-IL23 mice upon LPS stimulation.

We extended our observations in the chronic LPS-model. Here, lymphocytic infiltrates developed under the LPS-stimulus, which resembled the infiltrates we observed in much older non-LPS-treated GF-IL23 mice. Apparently, the LPS-stimulus accelerates the IL-23-driven CNS pathology in our transgenic mouse model. This was further confirmed by the increased mRNA-level of proinflammatory cytokines in GF-IL23 mice after chronic LPS-treatment. It is well known that endotoxemia and infections can induce and modulate the course of autoimmune diseases [66]. GF-IL23 mice will be a useful tool to examine the role of IL-23 as a link between infectious diseases and autoimmunity.

In conclusion, we established the GF-IL23 mouse model with a CNS-restricted IL-23 production. GF-IL23 mice developed a spontaneous phenotype with progressive ataxia, cerebral accumulation of inflammatory infiltrates with a high proportion of B cell, demyelination, and glial activation. Administration of LPS in GF-IL23 mice resulted in an early, pronounced microglial activation, enhanced cytokine production, and accelerated formation of lymphocytic infiltrates. The established GF-IL23 model is a promising tool to further study the influence of IL-23 in homeostasis and under various disease conditions, which is critical in the discovery of novel drug targets in neuroinflammatory disorders.

Acknowledgments We thank Marco Hessler for his expert technical assistance. We further thank Jens Reimann for his support in routine histological procedures. MM was a post-doctoral fellow from the Deutsche Forschungsgemeinschaft (DFG, Mu17-07/3-1) and was also supported by the fund 'Innovative Medical Research' of the University of Muenster Medical School, Germany. ILC was supported by a start-up grant from the University of Sydney. GCP was supported by grants from the European Union Joint Program, Neurodegenerative Disease Research program (JPND; Horizon 2020 Framework Programme, grant agreement 643417/DACAPO-AD) and a DZNE Intersite grant (DEMDAS 2). JZ was funded by the fund "Bonfor" from the University of Bonn Medical School, Germany and the DFG (KFO177, University of Bonn). LN was funded by the DFG (KFO177, University of Bonn) and the "Oppenheim Foerderpreis" Novartis GmbH.

Author Contributions Development of the transgenic construct: MM, MJH, ILC. Conceived and designed the experiments: LN, JZ, MK, MM. Performed the experiments: LN, JZ, MK, MM. Analyzed the data: LN, JZ, MK, AB, DG, MM. GCP planned and discussed the MRI experiments. RS developed and optimized the MRI sequences, performed the MRI experiments, analyzed the data, and wrote the MRI methods and results section. Contributed reagents/materials/analysis tools: LN, MTH, ILC, AB, DG, MM. Prepared the manuscript: LN, MM. Corrected and modified the manuscript: all authors.

Compliance with Ethical Standards

Ethical Approval All applicable national and institutional guidelines for the care and use of animals were followed. All animal experiments were approved by the Animal Care Commission of Nordrhein-Westfalen.

Conflict of Interest The authors declare that they have no conflict of interest.

LN and MM received travel grants from Merck, Sanofi Genzyme, TEVA, Novartis GmbH, honoraria for talks and research support from Novartis GmbH.

References

1. Becher B, Durell BG, Noelle RJ (2003) IL-23 produced by CNS-resident cells controls T cell encephalitogenicity during the effector phase of experimental autoimmune encephalomyelitis. J Clin Invest 112:1186–1191. https://doi.org/10.1172/JCI19079
2. Cua DJ, Sherlock J, Chen Y, Murphy CA, Joyce B, Seymour B, Lucian L, W T et al (2003) Interleukin-23 rather than interleukin-12 is the critical cytokine for autoimmune inflammation of the brain. Nature 421:744–748. https://doi.org/10.1038/nature01355
3. Alunno A, Carubbi F, Cafaro G, Pucci G, Battista F, Bartoloni E, Giacomelli R, Schillaci G et al (2015) Targeting the IL-23/IL-17 axis for the treatment of psoriasis and psoriatic arthritis. Expert Opin Biol Ther 15:1727–1737. https://doi.org/10.1517/14712598.2015.1084284
4. Cho JH, Feldman M (2015) Heterogeneity of autoimmune diseases: pathophysiologic insights from genetics and implications for new therapies. Nat Med 21:730–738. https://doi.org/10.1038/nm.3897
5. Fragoulis GE, Siebert S, McInnes IB (2016) Therapeutic targeting of IL-17 and IL-23 cytokines in immune-mediated diseases. Annu Rev Med 67:337–353. https://doi.org/10.1146/annurev-med-051914-021944
6. Furue M, Kadono T (2016) Psoriasis: behind the scenes. J Dermatol 43:4–8. https://doi.org/10.1111/1346-8138.13186
7. Zaky DS, El-Nahrery EM (2016) Role of interleukin-23 as a biomarker in rheumatoid arthritis patients and its correlation with disease activity. Int Immunopharmacol 31:105–108. https://doi.org/10.1016/j.intimp.2015.12.011
8. Javan MR, Shahraki S, Safa A, Zamani MR, Salmaninejad A, Aslani S (2017) An interleukin 12 B single nucleotide polymorphism increases IL-12p40 production and is associated with increased disease susceptibility in patients with relapsing-remitting multiple sclerosis. Neurol Res 39:435–441. https://doi.org/10.1080/01616412.2017.1301623
9. Sie C, Korn T, Mitsdoerffer M (2014) Th17 cells in central nervous system autoimmunity. Exp Neurol 262(Pt A):18–27. https://doi.org/10.1016/j.expneurol.2014.03.009
10. Kebir H, Ifergan I, Alvarez JI, Bernard M, Poirier J, Arbour N, Duquette P, Prat A (2009) Preferential recruitment of interferon-gamma-expressing TH17 cells in multiple sclerosis. Ann Neurol 66:390–402. https://doi.org/10.1002/ana.21748
11. Wen SR, Liu GJ, Feng RN, Gong FC, Zhong H, Duan SR, Bi S (2012) Increased levels of IL-23 and osteopontin in serum and cerebrospinal fluid of multiple sclerosis patients. J Neuroimmunol 244:94–96. https://doi.org/10.1016/j.jneuroim.2011.12.004
12. Langrish CL, Chen Y, Blumenschein WM, Mattson J, Basham B, Sedgwick JD, McClanahan T, Kastelein RA et al (2005) IL-23 drives a pathogenic T cell population that induces autoimmune inflammation. J Exp Med 201:233–240. https://doi.org/10.1084/jem.20041257
13. Shajarian M, Alsahebfosoul F, Etemadifar M, Sedaghat N, Shahbazi M, Firouzabadi FP, Dezashibi HM (2015) IL-23 plasma level measurement in relapsing remitting multiple sclerosis (RRMS) patients compared to healthy subjects. Immunol Investig 44:36–44. https://doi.org/10.3109/08820139.2014.930477
14. Hu Y, Zheng Y, Wu Y, Ni B, Shi S (2014) Imbalance between IL-17A-producing cells and regulatory T cells during ischemic stroke. Mediat Inflamm 2014:813045. https://doi.org/10.1155/2014/813045
15. Lv M, Liu Y, Zhang J, Sun L, Liu Z, Zhang S, Wang B, Su D et al (2011) Roles of inflammation response in microglia cell through Toll-like receptors 2/interleukin-23/interleukin-17 pathway in cerebral ischemia/reperfusion injury. Neuroscience 176:162–172. https://doi.org/10.1016/j.neuroscience.2010.11.066
16. Shichita T, Sugiyama Y, Ooboshi H, Sugimori H, Nakagawa R, Takada I, Iwaki T, Okada Y et al (2009) Pivotal role of cerebral interleukin-17-producing gamma deltaT cells in the delayed phase of ischemic brain injury. Nat Med 15:946–950. https://doi.org/10.1038/nm.1999
17. Wang M, Zhong D, Zheng Y, Li H, Chen H, Ma S, Sun Y, Yan W et al (2015) Damage effect of interleukin (IL)-23 on oxygen-glucose-deprived cells of the neurovascular unit via IL-23 receptor. Neuroscience 289:406–416. https://doi.org/10.1016/j.neuroscience.2015.01.012
18. Zheng Y, Zhong D, Chen H, Ma S, Sun Y, Wang M, Liu Q, Li G (2015) Pivotal role of cerebral interleukin-23 during immunologic injury in delayed cerebral ischemia in mice. Neuroscience 290:321–331. https://doi.org/10.1016/j.neuroscience.2015.01.041
19. Abbas A, Gregersen I, Holm S, Daissormont I, Bjerkeli V, Krohg-Sørensen K, Skagen KR, Dahl TB et al (2015) Interleukin 23 levels are increased in carotid atherosclerosis: possible role for the interleukin 23/interleukin 17 axis. Stroke 46:793–799. https://doi.org/10.1161/STROKEAHA.114.006516
20. Vom Berg J, Prokop S, Miller KR, Obst J, Kälin RE, Lopategui-Cabezas I, Wegner A, Mair F et al (2012) Inhibition of IL-12/IL-23 signaling reduces Alzheimer's disease-like pathology and cognitive decline. Nat Med 18:1812–1819. https://doi.org/10.1038/nm.2965
21. Town T, Bai F, Wang T, Kaplan AT, Qian F, Montgomery RR, Anderson JF, Flavell RA et al (2009) Toll-like receptor 7 mitigates lethal West Nile encephalitis via interleukin 23-dependent immune

cell infiltration and homing. Immunity 30:242–253. https://doi.org/10.1016/j.immuni.2008.11.012
22. Oppmann B, Lesley R, Blom B, Timans JC, Xu Y, Hunte B, Vega F, Yu N et al (2000) Novel p19 protein engages IL-12p40 to form a cytokine, IL-23, with biological activities similar as well as distinct from IL-12. Immunity 13:715–725
23. Parham C, Chirica M, Timans J, Vaisberg E, Travis M, Cheung J, Pflanz S, Zhang R et al (2002) A receptor for the heterodimeric cytokine IL-23 is composed of IL-12Rbeta1 and a novel cytokine receptor subunit, IL-23R. J Immunol 168:5699–5708
24. Pirhonen J, Matikainen S, Julkunen I (2002) Regulation of virus-induced IL-12 and IL-23 expression in human macrophages. J Immunol 169:5673–5678
25. Bettelli E, Carrier Y, Gao W, Korn T, Strom TB, Oukka M, Weiner HL, Kuchroo VK (2006) Reciprocal developmental pathways for the generation of pathogenic effector TH17 and regulatory T cells. Nature 441:235–238. https://doi.org/10.1038/nature04753
26. Mangan PR, Harrington LE, O'Quinn DB, Helms WS, Bullard DC, Elson CO, Hatton RD, Wahl SM et al (2006) Transforming growth factor-beta induces development of the T(H)17 lineage. Nature 441:231–234. https://doi.org/10.1038/nature04754
27. Veldhoen M, Hocking RJ, Atkins CJ, Locksley RM, Stockinger B (2006) TGFbeta in the context of an inflammatory cytokine milieu supports de novo differentiation of IL-17-producing T cells. Immunity 24:179–189. https://doi.org/10.1016/j.immuni.2006.01.001
28. Haak S, Croxford AL, Kreymborg K, Heppner FL, Pouly S, Becher B, Waisman A (2009) IL-17A and IL-17F do not contribute vitally to autoimmune neuro-inflammation in mice. J Clin Invest 119:61–69. https://doi.org/10.1172/JCI35997
29. Komiyama Y, Nakae S, Matsuki T, Nambu A, Ishigame H, Kakuta S, Sudo K, Iwakura Y (2006) IL-17 plays an important role in the development of experimental autoimmune encephalomyelitis. J Immunol 177:566–573
30. Kreymborg K, Etzensperger R, Dumoutier L, Haak S, Rebollo A, Buch T, Heppner FL, Renauld JC et al (2007) IL-22 is expressed by Th17 cells in an IL-23-dependent fashion, but not required for the development of autoimmune encephalomyelitis. J Immunol 179:8098–8104
31. Codarri L, Gyülvészi G, Tosevski V, Hesske L, Fontana A, Magnenat L, Suter T, Becher B (2011) RORγt drives production of the cytokine GM-CSF in helper T cells, which is essential for the effector phase of autoimmune neuroinflammation. Nat Immunol 12:560–567. https://doi.org/10.1038/ni.2027
32. McQualter JL, Darwiche R, Ewing C, Onuki M, Kay TW, Hamilton JA, Reid HH, Bernard CC (2001) Granulocyte macrophage colony-stimulating factor: a new putative therapeutic target in multiple sclerosis. J Exp Med 194:873–882
33. Akwa Y, Hassett DE, Eloranta ML, Sandberg K, Masliah E, Powell H, Whitton JL, Bloom FE et al (1998) Transgenic expression of IFN-alpha in the central nervous system of mice protects against lethal neurotropic viral infection but induces inflammation and neurodegeneration. J Immunol 161:5016–5026
34. Campbell IL, Abraham CR, Masliah E, Kemper P, Inglis JD, Oldstone MB, Mucke L (1993) Neurologic disease induced in transgenic mice by cerebral overexpression of interleukin 6. Proc Natl Acad Sci U S A 90:10061–10065
35. Pagenstecher A, Lassmann S, Carson MJ, Kincaid CL, Stalder AK, Campbell IL (2000) Astrocyte-targeted expression of IL-12 induces active cellular immune responses in the central nervous system and modulates experimental allergic encephalomyelitis. J Immunol 164:4481–4492
36. Zimmermann J, Krauthausen M, Hofer MJ, Heneka MT, Campbell IL, Müller M (2013) CNS-targeted production of IL-17A induces glial activation, microvascular pathology and enhances the neuroinflammatory response to systemic endotoxemia. PLoS One 8:e57307. https://doi.org/10.1371/journal.pone.0057307
37. Boztug K, Carson MJ, Pham-Mitchell N, Asensio VC, DeMartino J, Campbell IL (2002) Leukocyte infiltration, but not neurodegeneration, in the CNS of transgenic mice with astrocyte production of the CXC chemokine ligand 10. J Immunol 169:1505–1515
38. Metten P, Best KL, Cameron AJ, Saultz AB, Zuraw JM, Yu CH, Wahlsten D, Crabbe JC (2004) Observer-rated ataxia: rating scales for assessment of genetic differences in ethanol-induced intoxication in mice. J Appl Physiol (1985) 97:360–368. https://doi.org/10.1152/japplphysiol.00086.2004
39. Quintana A, Müller M, Frausto RF, Ramos R, Getts DR, Sanz E, Hofer MJ, Krauthausen M et al (2009) Site-specific production of IL-6 in the central nervous system retargets and enhances the inflammatory response in experimental autoimmune encephalomyelitis. J Immunol 183:2079–2088. https://doi.org/10.4049/jimmunol.0900242
40. de Haas AH, Boddeke HW, Biber K (2008) Region-specific expression of immunoregulatory proteins on microglia in the healthy CNS. Glia 56:888–894. https://doi.org/10.1002/glia.20663
41. Bodea LG, Wang Y, Linnartz-Gerlach B, Kopatz J, Sinkkonen L, Musgrove R, Kaoma T, Muller A et al (2014) Neurodegeneration by activation of the microglial complement-phagosome pathway. J Neurosci 34:8546–8556. https://doi.org/10.1523/JNEUROSCI.5002-13.2014
42. Dong R, Hu D, Yang Y, Chen Z, Fu M, Wang DW, Xu X, Tu L (2017) EETs reduces LPS-induced hyperpermeability by targeting GRP78 mediated Src activation and subsequent Rho/ROCK signaling pathway. Oncotarget 8:50958–50971. https://doi.org/10.18632/oncotarget.17331
43. Li CC, Munitic I, Mittelstadt PR, Castro E, Ashwell JD (2015) Suppression of dendritic cell-derived IL-12 by endogenous glucocorticoids is protective in LPS-induced sepsis. PLoS Biol 13:e1002269. https://doi.org/10.1371/journal.pbio.1002269
44. Hauser SL, Bar-Or A, Comi G, Giovannoni G, Hartung HP, Hemmer B, Lublin F, Montalban X et al (2017) Ocrelizumab versus interferon Beta-1a in relapsing multiple sclerosis. N Engl J Med 376:221–234. https://doi.org/10.1056/NEJMoa1601277
45. Li R, Bar-Or A (2018) The multiple roles of B cells in multiple sclerosis and their implications in multiple sclerosis therapies. Cold Spring Harb Perspect Med 9. https://doi.org/10.1101/cshperspect.a029108
46. Li R, Patterson KR, Bar-Or A (2018) Reassessing B cell contributions in multiple sclerosis. Nat Immunol 19:696–707. https://doi.org/10.1038/s41590-018-0135-x
47. Pöllinger B, Krishnamoorthy G, Berer K, Lassmann H, Bösl MR, Dunn R, Domingues HS, Holz A et al (2009) Spontaneous relapsing-remitting EAE in the SJL/J mouse: MOG-reactive transgenic T cells recruit endogenous MOG-specific B cells. J Exp Med 206:1303–1316. https://doi.org/10.1084/jem.20090299
48. Batista FD, Harwood NE (2009) The who, how and where of antigen presentation to B cells. Nat Rev Immunol 9:15–27. https://doi.org/10.1038/nri2454
49. Crawford A, Macleod M, Schumacher T, Corlett L, Gray D (2006) Primary T cell expansion and differentiation in vivo requires antigen presentation by B cells. J Immunol 176:3498–3506
50. McLaughlin KA, Wucherpfennig KW (2008) B cells and autoantibodies in the pathogenesis of multiple sclerosis and related inflammatory demyelinating diseases. Adv Immunol 98:121–149. https://doi.org/10.1016/S0065-2776(08)00404-5
51. Ferretti E, Ponzoni M, Doglioni C, Pistoia V (2016) IL-17 superfamily cytokines modulate normal germinal center B cell migration. J Leukoc Biol 100:913–918. https://doi.org/10.1189/jlb.1VMR0216-096RR
52. Luther SA, Lopez T, Bai W, Hanahan D, Cyster JG (2000) BLC expression in pancreatic islets causes B cell recruitment and

lymphotoxin-dependent lymphoid neogenesis. Immunity 12:471–481
53. Phares TW, DiSano KD, Stohlman SA, Segal BM, Bergmann CC (2016) CXCL13 promotes isotype-switched B cell accumulation to the central nervous system during viral encephalomyelitis. Brain Behav Immun 54:128–139. https://doi.org/10.1016/j.bbi.2016.01.016
54. Mitsdoerffer M, Lee Y, Jäger A, Kim HJ, Korn T, Kolls JK, Cantor H, Bettelli E et al (2010) Proinflammatory T helper type 17 cells are effective B-cell helpers. Proc Natl Acad Sci U S A 107:14292–14297. https://doi.org/10.1073/pnas.1009234107
55. Pfeifle R, Rothe T, Ipseiz N, Scherer HU, Culemann S, Harre U, Ackermann JA, Seefried M et al (2017) Regulation of autoantibody activity by the IL-23-TH17 axis determines the onset of autoimmune disease. Nat Immunol 18:104–113. https://doi.org/10.1038/ni.3579
57. Chognard G, Bellemare L, Pelletier AN, Dominguez-Punaro MC, Beauchamp C, Guyon MJ, Charron G, Morin N et al (2014) The dichotomous pattern of IL-12r and IL-23R expression elucidates the role of IL-12 and IL-23 in inflammation. PLoS One 9:e89092. https://doi.org/10.1371/journal.pone.0089092
56. Cocco C, Morandi F, Airoldi I (2011) Interleukin-27 and interleukin-23 modulate human plasmacell functions. J Leukoc Biol 89:729–734. https://doi.org/10.1189/jlb.1210660
58. Harbour SN, Maynard CL, Zindl CL, Schoeb TR, Weaver CT (2015) Th17 cells give rise to Th1 cells that are required for the pathogenesis of colitis. Proc Natl Acad Sci U S A 112:7061–7066. https://doi.org/10.1073/pnas.1415675112
59. Hirota K, Duarte JH, Veldhoen M, Hornsby E, Li Y, Cua DJ, Ahlfors H, Wilhelm C et al (2011) Fate mapping of IL-17-producing T cells in inflammatory responses. Nat Immunol 12:255–263. https://doi.org/10.1038/ni.1993
60. Kurschus FC, Croxford AL, Heinen AP, Wörtge S, Ielo D, Waisman A (2010) Genetic proof for the transient nature of the Th17 phenotype. Eur J Immunol 40:3336–3346. https://doi.org/10.1002/eji.201040755
61. Ahern PP, Schiering C, Buonocore S, McGeachy MJ, Cua DJ, Maloy KJ, Powrie F (2010) Interleukin-23 drives intestinal inflammation through direct activity on T cells. Immunity 33:279–288. https://doi.org/10.1016/j.immuni.2010.08.010
62. Annunziato F, Cosmi L, Santarlasci V, Maggi L, Liotta F, Mazzinghi B, Parente E, Filì L et al (2007) Phenotypic and functional features of human Th17 cells. J Exp Med 204:1849–1861. https://doi.org/10.1084/jem.20070663
63. Ip JP, Noçon AL, Hofer MJ, Lim SL, Müller M, Campbell IL (2011) Lipocalin 2 in the central nervous system host response to systemic lipopolysaccharide administration. J Neuroinflammation 8:124. https://doi.org/10.1186/1742-2094-8-124
64. Kawanokuchi J, Shimizu K, Nitta A, Yamada K, Mizuno T, Takeuchi H, Suzumura A (2008) Production and functions of IL-17 in microglia. J Neuroimmunol 194:54–61. https://doi.org/10.1016/j.jneuroim.2007.11.006
65. Sonobe Y, Liang J, Jin S, Zhang G, Takeuchi H, Mizuno T, Suzumura A (2008) Microglia express a functional receptor for interleukin-23. Biochem Biophys Res Commun 370:129–133. https://doi.org/10.1016/j.bbrc.2008.03.059
66. Kivity S, Agmon-Levin N, Blank M, Shoenfeld Y (2009) Infections and autoimmunity–friends or foes? Trends Immunol 30:409–414. https://doi.org/10.1016/j.it.2009.05.005